Dominance for Vestibular Cortical Function in the Non-dominant Hemisphere

M. Dieterich, S. Bense, S. Lutz[1], A. Drzezga[1], T. Stephan[2], P. Bartenstein[1,3] and T. Brandt[2]

Department of Neurology, Johannes Gutenberg-University, Mainz, [1]Department of Nuclear Medicine, Technical University Munich, [2]Department of Neurology, Ludwig-Maximilians-University, Munich and [3]Department of Nuclear Medicine, Johannes Gutenberg-University, Mainz, Germany

The aim of this ^{15}O-labelled H_2O bolus positron emission tomography (PET) study was to analyse the hemispheric dominance of the vestibular cortical system. Therefore, the differential effects of caloric vestibular stimulation (right or left ear irrigation with warm water at 44°C) on cortical and subcortical activation were studied in 12 right-handed and 12 left-handed healthy volunteers. Caloric irrigation induces a direction-specific sensation of rotation and nystagmus. Significant regional cerebral blood flow increases were found in a network within both hemispheres, including the superior frontal gyrus/sulcus, the precentral gyrus and the inferior parietal lobule with the supramarginal gyrus. These areas correspond best to the cortical ocular motor centres, namely the prefrontal cortex, the frontal eye field and the parietal eye field, known to be involved in the processing of caloric nystagmus. Furthermore, distinct temporo-parietal activations could be separated in the posterior part of the insula with the adjacent superior temporal gyrus, the inferior parietal lobule and precuneus. These areas fit best to the human homologues of multisensory vestibular cortex areas identified in the monkey and correspond to the parieto-insular vestibular cortex (PIVC), the visual temporal sylvian area (VTS) and areas 7 and 6. Further cortical activations were seen in the anterior insula, the inferior frontal gyrus and anterior cingulum. The subcortical activation pattern in the putamen, thalamus and midbrain is consistent with the organization of efferent ocular motor pathways. Cortical and subcortical activation of the described areas was bilateral during monaural stimulation, but predominant in the hemisphere ipsilateral to the stimulated ear and exhibited a significant right hemispheric dominance for vestibular and ocular motor structures in right-handed volunteers. Similarly, a significant left hemispheric dominance was found in the 12 left-handed volunteers. Thus, this PET study showed for the first time that cortical and subcortical activation by vestibular caloric stimulation depends (i) on the handedness of the subjects and (ii) on the side of the stimulated ear. Maximum activation was therefore found when the non-dominant hemisphere was ipsilateral to the stimulated ear, i.e. in the right hemisphere of right-handed subjects during caloric irrigation of the right ear and in the left hemisphere of left-handed subjects during caloric irrigation of the left ear. The localization of handedness and vestibular dominance in opposite hemispheres might conceivably indicate that the vestibular system and its hemispheric dominance, which matures earlier during ontogenesis, determine right- or left-handedness.

Introduction

Animal studies have identified several distinct and separate areas of the parietal and temporal cortex which receive vestibular afferents, e.g. area 2v at the tip of the intraparietal sulcus (Fredrickson *et al.*, 1966; Schwarz and Fredrickson, 1971; Büttner and Buettner, 1978), area 3aV (neck, trunk and vestibular region of area 3a) in the central sulcus (Phillips *et al.*, 1971; Schwarz *et al.*, 1973; Ödkvist *et al.*, 1974) and the parieto-insular vestibular cortex (PIVC) at the posterior end of the insula (Grüsser *et al.*, 1982, 1990a,b). Grüsser and co-workers found multisensory neurons in the PIVC of *Macaca fascicularis* which responded to (rotational) vestibular, somatosensory and optokinetic stimuli. These three vestibular cortical regions are closely connected to each other – as shown in tracer studies in squirrel monkeys – and are therefore named 'the inner vestibular cortical circle' (Guldin and Grüsser, 1996). Other regions interconnected with this 'inner circle' are the cingulum, the post arcuate area 6 (6pa), the granular insular region (Guldin and Grüsser, 1996), parts of areas 7 in the inferior parietal lobe (Ventre and Faugier-Grimaud, 1986; Faugier-Grimaud and Ventre, 1989) and a region posterior and adjacent to the PIVC cortex called the visual temporal sylvian area (VTS) (Guldin and Grüsser, 1996) or visual posterior sylvian area (VPS) (Guldin and Grüsser, 1998).

Current approaches that correlate brain structure and vestibular function include blood flow measurements with single-photon emission computed tomography (SPECT) (Friberg *et al.*, 1985; Takeda *et al.*, 1996), functional magnetic resonance imaging (fMRI) (Lobel *et al.*, 1998; Bense *et al.*, 2001; Suzuki *et al.*, 2001) and positron emission tomography (PET) (Bottini *et al.*, 1994, 2001; Wenzel *et al.*, 1996). Of these attempts to delineate the several human vestibular cortex areas to date, PET activation studies with caloric irrigation and fMRI activation studies with galvanic stimulation at the mastoid level have yielded the most detailed information. Bottini and co-workers (Bottini *et al.*, 1994), using caloric irrigation with iced water, were the first to demonstrate widespread activation in only the contralateral temporo-parietal junction, the posterior insula, the putamen and the anterior cingulate cortex, as well as the primary sensory cortex. Their data were based on caloric irrigation of one ear using painfully iced water. Recently, more distinct and separate activations in fMRI could be delineated during galvanic (electric) stimulation (Lobel *et al.*, 1998; Bense *et al.*, 2001) or caloric irrigation (Suzuki *et al.*, 2001) of both vestibular nerves. By this means, a network of cortical areas similar to that found in monkeys was detected. This network included areas in the parieto-occipital-temporal region of the parietal cortex (area 7), the insula and retroinsular regions (PIVC and VTS), the superior parietal lobe (possibly area 2v), the intraparietal sulcus, the central sulcus and the frontal premotor cortex. The areas were distributed in both hemispheres, but there was probably a predominance of the temporo-parietal areas of the right hemisphere in the right-handed normal subjects (Bense *et al.*, 2001), especially of intraparietal sulcus activation (Suzuki *et al.*, 2001). This seems to be in contrast to the mainly contralateral activation described by Bottini and co-workers (Bottini *et al.*, 1994). However, due to the methodological limitations of bilateral galvanic stimulation (Bense *et al.*, 2001), which did not allow analysis of the activation pattern during stimulation of one vestibular nerve, some open questions deserved further clarification, especially those with respect to hemispheric dominance:

- which cortical and subcortical areas are regularly activated during monaural caloric vestibular stimulation and how are they related to the neurophysiologically determined vestibular projections delineated in non-human primates?
- does monaural stimulation cause symmetrical activations in both hemispheres, or an activation predominantly in the contralateral hemisphere?
- is there hemispheric dominance of vestibular cortex areas?
- if there is hemispheric dominance, how does this interact with a mainly contralateral projection? Which effect is stronger?

Therefore, we studied the activation pattern during vestibular irrigation of the right or left ear with non-painful warm water (44°C) in 12 right-handed and 12 left-handed healthy volunteers.

Materials and Methods

Experimental Subjects

Twelve healthy right-handed volunteers aged 30–61 years (mean age 42.4 years, three women and nine men) and 12 healthy male volunteers with pronounced left-handedness aged 19–43 years (mean age 27.6 years) participated in the study. None of the subjects had any history or complaints of neurological or otoneurological dysfunction. The Laterality Quotient for right-handedness according to the 10-item inventory of the Edinburgh test (Oldfield, 1971; Salmaso and Longoni, 1985) was +100 in 10 of the 12 right-handed volunteers, +80 in one and +60 in the other one. The Laterality Quotient for left-handedness was –100 in 10 and –80 in two of the 12 left-handed volunteers. In accordance with the Declaration of Helsinki, all subjects gave their informed written consent to participate in the study, after the experimental procedure and radiation risks had been explained. The experiment had the approval of the Ethics Committee of the Technical University Munich and the Radiation Safety Authorities.

Caloric Irrigation and Electro-oculography

Vestibular stimulation was performed by irrigating the right or left ear canals with 100 ml of warm water at 44°C for ~50 s. A 100 ml syringe was used in conjunction with a flexible plastic tube placed in the external auditory meatus of each ear. The head was slightly elevated (20°) for optimum stimulation of the horizontal canal. To monitor the effects, the horizontal DC electro-oculogram was recorded with the help of two cup electrodes placed at the lateral canthi of each eye (ground electrode over the glabella). For calibration purposes, the subject was asked to look at targets 0 or 20° to the left and 20° to the right. The subjects kept their eyes closed during the control condition and during and after caloric irrigation. The slow phase velocity (SPV) of the caloric nystagmus was analysed at the end of caloric irrigation and during the scanning period. After the scans, the subjects were asked to comment on their perception of motion. The subjective strength of the vestibular sensation was quantified by determining the perceived intensity of body rotation on a visual analogue scale (VAS, 0–10).

Experimental Setup

The 12 right-handed and 12 left-handed healthy volunteers were tested – with eyes closed – during vestibular stimulation by irrigating the right or left ear canals with 100 ml of warm water at 44°C for 50 s. The control condition was a rest condition defined as lying supine with eyes closed and without stimulation.

PET – Scanning and Data Acquisition

PET measurements were performed using a Siemens 951 R/31 PET scanner (CTI, Knoxville TN) with a total axial field of view of 10.5 cm and no inter-plane dead space. In this field of view, the brain areas covered in all subjects extended from the vertex to the upper cerebellum. Attenuation correction was performed on an individual basis using a transmission scan with an external 68Ge/68Ga ring source acquired prior to the tracer injection.

The emission data were sampled in 3D mode for each subject under the three conditions mentioned above: irrigation of one ear (B), of the other ear (C) and the absence of such stimulation (A). Each condition was repeated up to four times (typical configuration ABCCBAACBBCA). The initial stimulation condition was thus varied in random order. To measure regional cerebral blood flow (rCBF), 10.0 mCi ^{15}O-labelled water were administered using a semibolus technique described previously (Drzezga *et al.*, 2001). To avoid the influence of nonvestibular effects of caloric stimulation (nociceptive, somatosensory and acoustic sensations), scans, which were sampled for 50 s, started 25 s after irrigation ended. Previous tests had revealed that nystagmus is still prominent at this time, but sensory sensations had already disappeared. A 10 min interval between the scans allowed for decay of radioactivity. The subjects were comfortably positioned on the scanner table to reduce movement artefacts during the relatively long scanning procedure (~3.5 h). Before each PET scan, the position of the subject's head was checked by laser pointer and position markers.

Image Analysis

Image analysis was performed on an UltraSPARC workstation (Sun Microsystems), using commercial interactive image display software and MATLAB (The MathWorks Inc., Natick, MA) for calculations and image matrix manipulations. To derive maps of significant blood flow changes on a pixelwise basis, statistical parametric mapping software (SPM99b; Wellcome Department of Cognitive Neurology, London, UK) was used (Friston *et al.*, 1995b).

After corrections for randoms, dead time and scatter, images were reconstructed by filtered back-projection with a Hanning filter (cut-off frequency 0.4 cycles/projection element), which resulted in 31 slices with a 128 × 128 pixel matrix (pixel size = 2.0 mm) and interplane separation of 3.375 mm. To correct for head movements between the scans, the images were realigned using the first image as a reference and subsequently spatially normalized (Friston *et al.*, 1995a) into a stereotaxic space using a representative brain from the Montreal Neurological Institute (MNI) as template. After normalization, the set of aligned images of each subject was compatible with the coordinate system proposed by Talairach and Tournoux (Talairach and Tournoux, 1988; Frackowiak *et al.*, 1997). To eliminate individual differences in gyral anatomy and brain size, as well as to supply a meaningful statistical comparison of regional signal changes across the groups, these images were further smoothed using an isotropic Gaussian kernel of 12 mm (FWHM).

To remove effects induced by variations in global flow across subjects and scans, an analysis of covariance (ANCOVA) was applied with global flow as the confounding variable (Friston *et al.*, 1995b). These adjusted rCBF voxel values were used for subsequent statistical analysis. Comparisons across stimulus conditions (calorics right or left) and baseline were made by Gaussionized *t*-statistics. Contrasts of parameter estimates were computed for each subject and written out as contrast images for the positive as well as for the negative signal changes (SPM manual page). Statistical parametric maps were created for each group of subjects by entering the contrast images from the first-level statistics into a *t*-test; this yielded a random effects model that allows inference to the general population (Frison and Popcock, 1992; Woods, 1996). Each resulting voxel set constitutes an SPM(*t*) map.

To implement a second-level analysis of laterality effects (hemispheric dominance), the subject-specific contrast images were flipped across the midline. Then, the flipped and non-flipped images were entered as two groups into a paired *t*-test. To test for jointly activated areas during right and left-sided caloric irrigation within one subject group (conjunction analysis), we entered contrasts for the two groups as different effects at the second level and performed a conjunction of contrasts testing for each alone (simple regression analysis).

On the basis of previous studies (Bottini *et al.*, 1994; Wenzel *et al.*, 1996; Bense *et al.*, 2001), an anatomically constrained hypothesis was used and signal changes within the presumed vestibular and visual network (including posterior insular cortex), which were significant at $P < 0.001$ and not corrected for multiple comparisons, are reported throughout the paper. Similar hypothesis-driven approaches with identical thresholds have been applied in several other PET-imaging studies for their potential of reducing false negative findings (Spence *et al.*, 1997; Boecker *et al.*, 1999).

To define the anatomical sites of activation and deactivation clusters, MNI coordinates as well as defined anatomical landmarks (Naidich and

Table 1
Areas with signal increases during caloric vestibular stimulation of the right ear in right-handed volunteers obtained by statistical group analysis ($n = 12$)

Area	BA	Right hemisphere					Left hemisphere				
		T	*X*	*Y*	*Z*	Cluster	*T*	*X*	*Y*	*Z*	Cluster
Posterior, anterior insula	IV/IH	11.26	30	2	–8	2386	5.55	–34	0	–4	151
Putamen		10.06	26	–6	6		5.02	–42	–4	2	
Inf. frontal gyrus/anterior insula	46	7.82	38	36	6						
Postcentral gyrus	40	8.19	48	–26	24	1284					
Postcentral gyrus	40/42	7.12	56	–36	20		8.63	–66	–28	22	61
Inferior parietal lobule	40	6.81	64	–36	32		4.51	–72	–38	36	12
Anterior cingulum	32						7.34	–12	28	28	779
Anterior cingulum							6.63	–20	8	24	
Anterior cingulum							6.46	–14	14	28	
Superior frontal gyrus	10						6.02	–18	54	–6	31
Thalamus posterolateral		5.52	24	–24	6	121	4.26	–24	–26	14	5
Thalamus posterolateral		5.50	14	–26	10						
Thalamus posteromedial		4.89	6	–26	12						
Hippocampus		5.35	28	–42	–2	10					
Medial frontal gyrus	9	4.91	48	10	38	56					
Substantia nigra							4.49	–10	–16	–12	12
Precuneus	7	4.46	10	–30	48	3					

T-values, corresponding Brodmann areas (BA), MNI coordinates (*X/Y/Z*) and cluster sizes (in voxel) are given for both hemispheres.

Brightbill, 1996; Stephan *et al.* 1997; Yousry *et al.* 1997) and the atlas of Talairach and Tournoux (Talairach and Tournoux, 1988) were used. There is still no internationally agreed upon definition of insular and retroinsular regions available in the literature. The insula was anatomically divided into five gyri; three short (I–III) and two long insular gyri (IV, V) (Bense *et al.*, 2001). The region frontal to the central insular sulcus was defined as the anterior insula; it includes the short insular gyri (I–III). The region posterior to the central insular sulcus was defined as the posterior insula; it includes the first (IV) and second (V) long insular gyrus. The retroinsular territory was defined as the area posterior to the second long insular gyrus.

Results

Right-handed Volunteers, Caloric Irrigation of the Right Ear

Warm-water vestibular stimulation of the right ear caused a sensation of being tilted toward the left side and a caloric nystagmus to the left (direction of slow phase), with a mean slow phase velocity of 17.8°/s (SD = 7.7°/s). Regional blood flow increases were found in the right hemisphere in the following areas: a larger cluster (2386 voxels) covered the inferior posterior (long insular gyrus IV) and adjacent anterior insula (short insular gyrus III), the putamen and the anterior insula (small parts of the short insular gyrus I) with the adjacent inferior frontal gyrus (BA 47); another cluster (1284 voxels) covered the postcentral gyrus (BA 40/42) and the inferior parietal lobule (BA 40). Further activations were located in the posterolateral and posteromedial thalamus, hippocampus, medial frontal gyrus (BA 9), superior parietal lobule (BA 40/7) and precuneus (BA 7) (see Table 1 and Figs 1, 4 and 5).

Cerebral activation of the left hemisphere showed fewer and smaller clusters located in the postcentral gyrus (BA 40/42; 61 voxels), the inferior parietal lobule (BA 40; 12 voxels), the anterior cingulum (BA 32), the superior frontal gyrus (BA 10), the putamen with posterior insula (long insular gyrus IV; 151 voxels), the posterolateral thalamus and the substantia nigra of the midbrain. For details see Table 1.

Right-handed Volunteers, Caloric Irrigation of the Left Ear

Warm-water stimulation of the left ear caused a sensation of being tilted toward the opposite side and a caloric nystagmus during the scanning period to the right (direction of slow phase), with a mean slow phase velocity of 17.3°/s (SD = 5.4°/s). Areas significantly activated in the right hemisphere were in general smaller and less significant than those in the left hemisphere, except for the anterior cingulate gyrus (see Table 2 and Figs 1, 4 and 5). They were located in the retroinsular region, with the transverse temporal gyrus (Heschl; BA 41) and the adjacent superior temporal gyrus (BA 41), the putamen and the inferior parts of the posterior insula (long insular gyrus IV) at the border of the anterior insula (short insular gyrus III) centring around the central insular sulcus (485 voxels of the cluster). The cluster of highest significance (347 voxels) within the right hemisphere was in the anterior cingulate gyrus, which was contralateral to the irrigated ear.

Activations of the left hemisphere included the region of the anterior (short insular gyrus III) and posterior (long insular gyrus IV) insula in more inferior parts compared to the right side, as well as the inferior parietal lobule (BA 40) and the adjacent superior temporal gyrus (BA 22; 161 + 7 voxels). Minor frontal activation was seen in the left inferior frontal gyrus/precentral gyrus (BA 44/6). Thus, activations were larger and more frequent in the hemisphere ipsilateral to the irrigated ear. Results of this part of the experiment are summarized in Table 2.

Compared to the activation pattern during caloric irrigation of the right ear, activated areas of the temporo-insular and parietal cortex were smaller in both hemispheres and more frequently located within the ipsilateral left than the right hemisphere. Only activations of the anterior cingulum were dominated in the right hemisphere. During vestibular stimulation of the left ear, this pattern appeared in some aspects to be a 'mirror-image' of that elicited during vestibular stimulation of the right ear.

Left-handed Volunteers, Caloric Irrigation of the Left Ear

In the 12 healthy volunteers with left-handedness, stimulation of the ipsilateral left ear caused a caloric nystagmus to the right

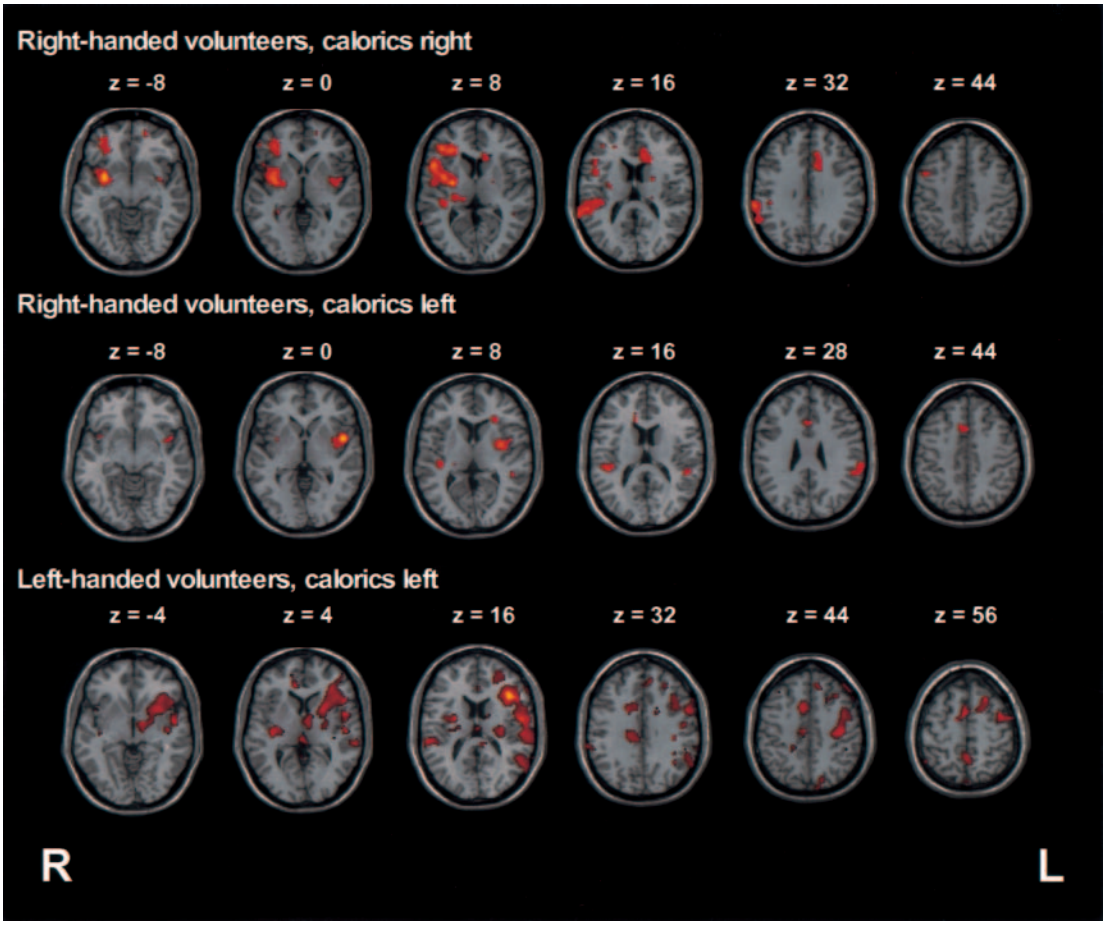

Figure 1. Areas activated during caloric stimulation of the right or left ear in right-handed and left-handed volunteers (group analysis; $n = 12$; $P < 0.001$). Activations were found in, for example, the anterior and posterior insula, the inferior frontal gyrus, the postcentral gyrus, the superior temporal gyrus, the inferior parietal lobule and the anterior cingulum. Note that activations were most pronounced in right-handers during caloric irrigation of the right ear in the right hemisphere and in left-handers during caloric irrigation of the left ear in the left hemisphere. Compared to the activation pattern during caloric irrigation of the right ear, caloric irrigation of the left ear in right-handers led to activations in the temporo-insular and parietal cortex which were smaller in both hemispheres and more frequently located within the left ipsilateral hemisphere.

(direction of slow phase), with a mean slow phase velocity of 11.3°/s (SD = ±3.5°/s). This was associated with a strong activation of the left hemisphere which covered an area including the anterior insula (I and II short insular gyri), the adjacent inferior frontal gyrus (BA 45), putamen, anterior thalamus, the posterior insula (long insular gyri IV and V), the transverse temporal gyrus (Heschl) and the postcentral gyrus (BA 43/4; see Table 3 and Figs 1, 4 and 5). This large activation cluster appeared to have ~7104 voxels. A smaller and separate activation of the left postcentral gyrus was located more rostrally (BA 4). Another cluster of activation was seen in the left superior temporal gyrus (BA 42/22), the adjacent inferior parietal lobule (BA 40) and the supramarginal gyrus (BA 40/39). Frontal premotor activation also occurred predominantly on the left side, including the medial frontal gyrus (BA 6/8) with the frontal eye field and the superior frontal gyrus (BA 8). There was bilateral parietal activation, left more than right, in the precuneus (BA 7). Only cingulate activation was predominant in the right contralateral hemisphere and located in its anterior part with a maximum in BA 24 and at the border of the supplementary motor area (BA 6).

Activations within the right hemisphere were smaller, separate and distinctly located in the region of the posterior (long insular gyri IV and V) and anterior (short insular gyri II and III) insula and did not extend into the frontal gyri (cluster size of comparable activations: 418 + 333 voxels versus 7104 voxels). Subcortical activation was observed in the putamen bilaterally and in the ipsilateral left anterior and paramedian thalamus (Fig. 1).

Left-handed Volunteers, Caloric Irrigation of the Right Ear

Warm-water stimulation of the right ear induced a caloric nystagmus to the left (direction of slow phase; mean slow phase velocity = 10.3 ± 3.7°/s) and was associated with several activations in both hemispheres which were distinct and separate with a maximal cluster size of 576 voxels (*T*-value = 14.04). Compared to the activations of the left-handed subjects during left-sided stimulation with a maximum cluster size of 7104 voxels (*T*-value 21.60) in the temporo-insular region, the activation pattern here appeared somewhat regularly scattered within both hemispheres. The small areas of activation within the right hemisphere included the diagonal frontal gyrus (BA 6), the precentral gyrus at two sites (BA 6 and BA 4/6) with the adjacent superior temporal gyrus (BA 22) and medial parts of the insula, rostral parts of the posterior insula (V), the precuneus (BA 7), the cingulate gyrus (BA 32) and the superior frontal (BA 10 and BA 6) and medial frontal (BA 46) gyri. Subcortical

Table 2
Areas with signal increases during caloric vestibular stimulation of the left ear in right-handed volunteers obtained by statistical group analysis ($n = 12$)

Area	BA	Right hemisphere					Left hemisphere				
		T	*X*	*Y*	*Z*	Cluster	*T*	*X*	*Y*	*Z*	Cluster
Anterior/posterior insula (central insular sulcus)	III/IV						11.07	–50	4	0	485
							6.56	–36	–2	8	
		4.40	42	10	–8	7	4.23	–38	4	–8	
Posterior insula/Heschl/GTs	retro/41	5.98	46	–34	16	161					
GTT (Heschl)	Heschi	5.59	40	–30	12						
Putamen		5.57	32	2	2	24					
Inferior parietal lobule	40						6.32	–64	–32	26	282
Superior temporal gyrus	22						5.73	–48	–38	10	
Inferior parietal lobule	40						4.93	–56	–40	24	
Anterior cingulum	32	8.80	6	18	36	347					
Ant. cingulum/corp. call.	24	5.35	12	26	16	11					
Ant. cingulum	32	4.85	14	36	22	16					
Inf. frontal gyrus/precentral g.	44/6						4.87	–46	2	24	9
Superior frontal gyrus	6						4.64	–20	10	72	16
Thalamus posterolateral		4.11	22	–26	8	2					

T-values, corresponding Brodmann areas (BA), MNI coordinates (*X/Y/Z*) and cluster sizes (in voxel) are given for both hemispheres. III = third short insular gyrus of the anterior insula; IV = first long insular gyrus of the posterior insula; retro = retroinsular; Heschl = Heschl's gyrus transverse temporal gyrus; corp. call. = corpus callosum.

Table 3
Areas with signal increases during caloric vestibular stimulation of the left ear in left-handed volunteers obtained by statistical group analysis ($n = 12$)

Area	BA	Right hemisphere					Left hemisphere				
		T	*X*	*Y*	*Z*	Cluster	*T*	*X*	*Y*	*Z*	Cluster
Anterior insula/GFi/putamen/anterior thalamus	45/I						21.60	–40	24	18	7104
GFi/anterior insula	45/I/II						18.63	–50	20	10	
Postcentral g./precentral g.	43/4						17.88	–56	–8	22	
Posterior insula/TTG	IV/V/41	22.48	36	–18	6	418	5.55	–34	0	–4	151
Putamen		8.68	26	–18	12		5.02	–42	–4	2	
Anterior insula	III	12.69	26	–4	16						
Anterior insula	III	5.11	44	8	0	11					
Anterior insula	II	4.93	30	14	10	17					
Superior temporal gyrus	42/22	14.66	52	–30	18	333	7.02	–54	–58	14	
Inferior parietal lobule	40	7.93	56	–38	28		7.15	–58	–64	24	662
Supramarginal gyrus	40/39						8.27	–40	–56	32	71
Inferior parietal lobule	40						5.30	–42	–40	38	
Superior parietal lobule	40	5.76	52	–56	54	46					
Anterior cingulum	32/24	13.46	10	38	2	54					
Anterior cingulum	24	11.82	12	12	36	655					
Anterior cingulum/GFd	6	11.12	2	4	56						
GFd	6	9.93	8	–2	60						
Cingulate gyrus	23	6.78	16	–22	34	340					
Corp. Call.							10.76	–2	–32	6	128
Superior frontal gyrus	8						10.45	–10	38	42	182
Gfd							7.69	–6	40	28	
Medial frontal gyrus	6						8.53	–26	20	52	308
Medial frontal gyrus	8						6.16	–34	26	44	
Precuneus	7						8.22	–10	–70	62	257
Precuneus	7	5.95	4	–46	50		7.46	–2	–50	58	
Precuneus	7						5.54	–16	–76	44	48
Precuneus/lobus paracentralis	7	7.39	16	–40	54						
Precuneus/lobus paracentralis	7	5.18	18	–38	46						
Postcentral gyrus	4 (3?)						6.09	–26	–34	66	40

T-values, corresponding Brodmann areas (BA), MNI coordinates (*X/Y/Z*) and cluster sizes (in voxel) are given for both hemispheres. I, II, III = anterior insula with the first, second, third short insular gyrus; IV,V = posterior insula with the first (IV) and second (V) long insular gyri; GFi = inferior frontal gyrus; GFd = medial frontal gyrus; TTG = transverse temporal gyrus (Heschl).

activations were seen in the paramedian and anterior-median thalamus, putamen and caudate nucleus.

Similar locations were found for the activations in the left hemisphere: diagonal and superior frontal gyrus (BA 6 and BA 8), precuneus (BA 7), rostral parts of the posterior insula (V), superior temporal gyrus (BA 42), medial frontal gyrus (BA 9/46) with the adjacent anterior parts of the insula, cingulate gyrus (BA 32), medial frontal gyrus (BA 9) and inferior frontal–precentral gyri (BA 44/6). Subcortical activations were also located in the anterior-median thalamus and the putamen.

The most pronounced activation was in the left hemisphere – with a *T*-value of 14.04 and the largest cluster size of 576 voxels

Table 4
Areas with signal increases during caloric vestibular stimulation of the right ear in left-handed volunteers obtained by statistical group analysis (n=12)

Area	BA	Right hemisphere					Left hemisphere				
		T	*X*	*Y*	*Z*	Cluster	*T*	*X*	*Y*	*Z*	Cluster
Posterior insula	V	9.55	36	–22	20	129	9.84	–40	–32	20	230
		7.63	38	–26	12		5.63	–32	–34	4	
Medial insula	45/1						4.13	–44	8	4	
Anterior insula	II	7.92	38	14	4	79					
Anterior rostral insula							7.35	–38	–10	20	106
Putamen/Caudate nucleus		7.57	24	–4	–6	126	7.83	–16	–4	6	298
		5.91	14	–18	–4		5.60	–10	4	10	
Medial thalamus		5.16	14	–16	16	26	14.16	–2	–24	2	266
Sup./diagonal frontal gyrus	6	14.04	12	4	52	576	12.70	–2	–26	58	121
Diagonal frontal gyrus	6	8.25	4	–16	78	15					
Superior frontal gyrus	6						6.09	–12	0	76	70
Precentral gyrus	6/44	6.63	58	4	30	111	12.58	–50	–4	8	125
Superior temporal gyrus	22						4.48	–54	4	2	
	22						5.89	–64	–46	20	24
Precentral gyrus	44/6	4.90	60	12	10	20					
Precentral gyrus	4/6						8.13	–50	–16	44	75
Superior temporal gyrus	42	8.53	66	–30	14	261					
Precuneus	7	12.76	4	–66	66	121	8.40	–14	–68	54	48
Superior frontal gyrus	8	8.19	22	46	50	16					
Medial frontal gyrus	9/46	7.99	26	40	18	174	7.10	–40	32	32	84
Medial frontal gyrus	9	5.60	58	6	42	111					
Anterior cingulum	32						7.35	–12	8	44	125
	24	6.77	16	20	28	71					
Superior parietal lobule	7	6.32	48	–66	54	12					
	7	5.49	22	–52	70	18					

T-values, corresponding Brodmann areas (BA), MNI coordinates (*X*/*Y*/*Z*) and cluster sizes (in voxel) are given for both hemispheres.

Table 5
Areas with signal increases during caloric vestibular stimulation when the images were flipped across the midline and the flipped and non-flipped images were entered as two groups into a paired t-test (group analysis, $n = 12$; $P \leq 0.001$)

Area	BA	Right hemisphere					Left hemisphere				
		T	*X*	*Y*	*Z*	Cluster	*T*	*X*	*Y*	*Z*	Cluster
Right–handed volunteers, calorics right											
Postcentral gyrus	2/40	11.49	62	–26	50	38					
Inferior frontal gyrus/ anterior insula	44/45	10.88	32	36	2	518					
Anterior cingulum	24						9.18	–8	26	20	718
Medial frontal gyrus	9	7.20	52	4	40	554					
Medial/superior frontal gyrus	9/46	7.07	28	38	28	159					
Inferior parietal lobule	40	6.79	58	–40	24	251					
Inferior parietal lobule	40	6.53	46	–40	44	269					
Superior parietal lobule	7	6.47	28	–58	68	26					
Inferior frontal gyrus	44	5.95	56	6	22	134					
Hippocampus	27/30						4.86	–14	–42	–4	14
Left–handed volunteers, calorics left											
Inferior parietal lobule	40						15.21	–44	–42	44	4264
Thalamus/caudate nucleus							14.45	–14	–36	10	160
Cuneus	19						12.95	–16	–88	36	190
Cuneus/medial occipital gyrus	19/18	9.78	16	–72	22	90					
Diagonal/medial frontal gyrus	8/6						8.51	–18	8	52	226
Anterior cingulum	24	8.11	10	–16	40	108	7.64	–2	44	28	67
	32	5.80	2	18	44	206					
Precentral gyrus	4/6						7.02	–20	–30	60	58
Medial temporal gyrus	19/39	6.48	44	–84	18	62					
Anterior insula	II/III	6.33	36	–2	16	43					
Precentral/medial frontal gyrus	6/9						6.03	–40	2	38	53
Posterior insula/sup. temp. gyrus	IV/V/22						5.96	–46	0	–6	136
Putamen							5.85	–28	12	6	31
Superior frontal gyrus	10	5.53	12	54	4	20					

– and covered the left superior and diagonal frontal gyrus (BA 6). The most pronounced cortical activation of the right hemisphere was in the superior temporal gyrus (BA 42; voxel size 261). A summary is given in Table 4.

Comparison of Both Hemispheres in Right- and Left-handed Volunteers

To compare the activation pattern in the right and left hemispheres in each group of handedness, the subject-specific

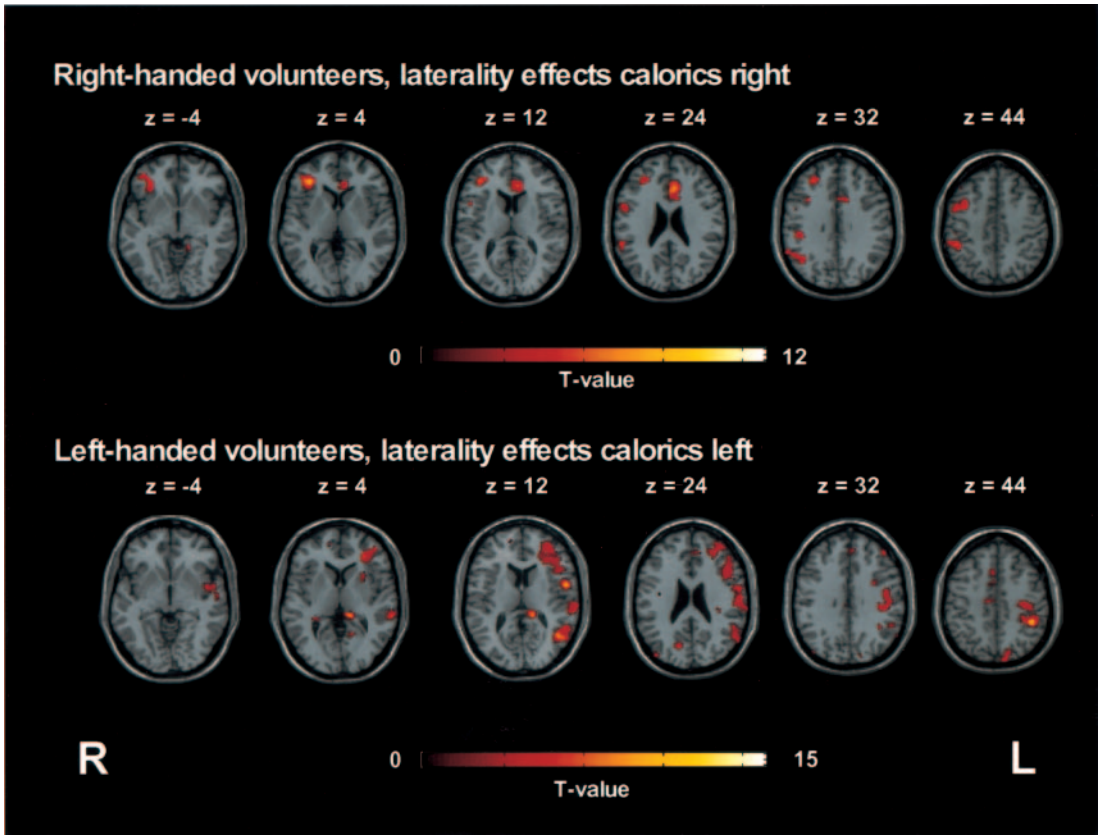

Figure 2. Comparison of both hemispheres in right- and left-handed volunteers (subject-specific contrast images were flipped across the midline and then the flipped and non-flipped images were entered as two groups into a paired *t*-test). During caloric irrigation of the right ear in right-handers, activations were pronounced in the right hemisphere, whereas activations were pronounced in the left hemisphere in left-handers during caloric stimulation of the left ear (for details, see Table 5). These data provide evidence for a hemispheric dominance of the non-dominant hemisphere for vestibular projections.

contrast images were flipped across the midline and then the flipped and non-flipped images were entered as two groups into a paired *t*-test.

Right-handed Volunteers: Calorics Right (Table 5 and Fig. 2)
Activations were pronounced in the right hemisphere, which had a total number of ~1950 voxels in contrast to 732 voxels in the left hemisphere. The activations of the right hemisphere concentrated in the inferior frontal gyrus/anterior insula (BA 44/45 and BA 46), the superior frontal gyrus (BA 9/46), the medial frontal gyrus (BA 9/6/8), the inferior parietal lobule and supramarginal gyrus (BA 40) and the superior parietal lobule (BA 7), whereas activations of the left hemisphere centred mainly in the anterior cingulate gyrus (BA 24) and hippocampus.

Right-handed Volunteers: Calorics Left
Activations occurred mainly in the left hemisphere (136 voxels in total). In the right hemisphere (a total of 42 voxels) only activity in the anterior cingulum (BA 24; $T = 5.48$; $x = 10$, $y = 8$, $z = 34$; 30 voxels) and the precuneus (BA 7) survived. The cluster with the highest number of 94 voxels was located in the left medial frontal gyrus ($T = 5.48$;–38, 18, 30). Smaller activations were in the left diagonal frontal gyrus (BA 8/6) and the precentral gyrus (BA 6).

Left-handed Volunteers: Calorics Left (Table 5 and Fig. 2)
The activations were pronounced in the left hemisphere of left-handed volunteers and totalled ~5000 voxels compared to 550 voxels within the right hemisphere. While the largest activation clusters within the right hemisphere appeared in the anterior cingulum (BA 32/24) and the occipital lobe (cuneus and medial occipital gyrus; BA 19/18), those within the left hemisphere centred in the posterior insula, the anterior insula/inferior frontal gyrus, superior frontal gyrus, superior temporal gyrus, inferior and superior parietal lobule, the precentral gyrus and the putamen.

Left-handed Volunteers: Calorics Right
Activation clusters were significantly smaller than with caloric irrigation of the left ear and frequently scattered over both hemispheres (total number of voxels in the right hemisphere was ~450 and in the left hemisphere ~550). The 'largest' clusters were in the left hemisphere, located in the cuneus (BA 19; 173 voxels; $T = 7.34$; –12, –90, 28) and the anterior cingulum (BA 24; 97 voxels; $T = 10.08$; –8, 6, 28). Further left-sided activations were seen in the diagonal frontal gyrus (BA 9/32; 40 voxels; $T = 7.11$; –20, 38, 18), the lateral thalamus (41 voxels; $T = 8.36$; –20, –24, 18), upper parts of the posterior insula (30 voxels; $T = 7.08$; –30, –24, 18) and fronto-parietal areas such as the diagonal frontal gyrus (BA 6; 37 voxels; $T = 6.43$; –20, –18, 50).

In the right hemisphere, activations concentrated in the occipital gyrus (BA 19; 94 voxels; $T = 8.21$; 34, –78, 28), the cuneus (BA 19; 42 voxels; $T = 11.59$; 6, –70, 10), the inferior parietal lobule adjacent to the posterior insula (92 voxels; $T = 10.09$; 36, –12, 24), the superior frontal gyrus (BA 9; 80 voxels; $T = 7.36$; 14, 64, 30), inferior parts of the posterior insula (IV/V; 36 voxels; $T = 6.01$; 34, –6, –6), the precuneus (BA 7; 33 voxels;

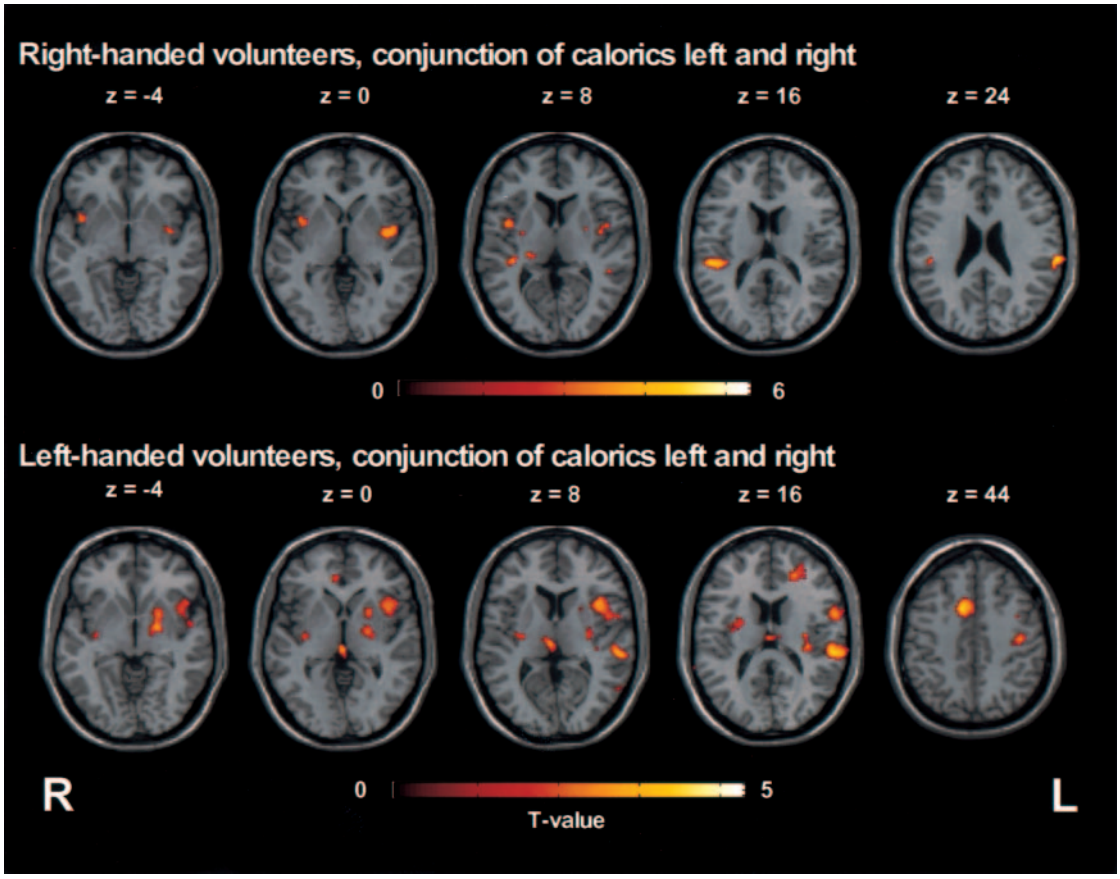

Figure 3. Conjunction analysis of caloric irrigations of the right and left ears for right- and left-handed volunteers. Activations appear in both hemispheres, especially in temporo-insular and parietal regions. A predominance of the non-dominant hemisphere can easily be observed in left-handed volunteers.

T = 5.28; 22, –70, 46), superior frontal gyrus (BA 8; 30 voxels; T = 7.31; 34, 36, 46) and the precentral gyrus (BA 6/44).

Conjunction Analysis

Right-handed Volunteers, Calorics Right versus Left ($P < 0.05$, Corrected for Multiple Comparisons; Fig. 3)

Activation areas that appeared under both conditions were located bilaterally in the posterior insula (III/IV right; IV/V left), the putamen, the superior temporal gyrus and inferior parietal lobule, as well as the right posterolateral thalamus and transverse temporal gyrus.

Additional areas with a lower significance level ($P \leq 0.001$, uncorrected) were seen. These included the anterior and posterior cingulum bilaterally, the superior temporal gyrus bilaterally with the adjacent right anterior insula, the superior frontal gyrus bilaterally, the left inferior frontal gyrus and left putamen, as well as the right medial frontal gyrus and right precuneus.

Left-handed Volunteers, Calorics Right versus Left ($P \leq 0.001$, Uncorrected; Fig. 3)

The largest clusters of activations under both conditions were found in the right anterior cingulum (BA 32; 832 voxels; T = 4.45; 10, 12, 42), the left inferior frontal gyrus (BA 44) with the adjacent superior temporal gyrus and anterior insula (831 voxels; T = 4.37; –58, 6, 32), the left superior temporal gyrus (BA 42/44; 415; T = 4.31; –58, –30, 12), the left (421; T = 3.57; –34, –26, 18) and right (294; T = 4.14; 34, –14, 22) upper parts of the posterior insula, the left medial frontal gyrus (BA 10; 324; T = 3.43; –32, 46, 22) and both diagonal frontal gyri (BA 6; T = 3.17; 10, 0, 64; T = 3.24; –12, 2, 70). Smaller activations occurred in the paramedian thalamus bilaterally, the left putamen and the left precuneus (BA 7).

Only the right anterior cingulum (T = 4.45), the left superior temporal gyrus (T = 4.37) and left inferior parietal lobule (T = 4.31), as well as the right posterior insula (T = 4.14) survived with a higher significance level ($P < 0.05$, corrected).

Discussion

Caloric vestibular stimulation of one ear activated a network of cortical and subcortical areas bilaterally, which caused different hemispheric asymmetries. These areas can be attributed to the multisensory vestibular cortical circuit and ocular motor areas. Quantitative activation was dependent (i) on hemispheric dominance for vestibular projections and (ii) on the ear (right or left) that was stimulated. Caloric irrigation of the right ear in right-handed volunteers and, even more so, of the left ear in left-handed volunteers, clearly showed that activated areas predominated in the non-dominant hemisphere. 'Mixed' stimulation conditions (e.g. stimulation of the left ear in right-handed subjects) demonstrated further that activation was stronger in the hemisphere ipsilateral to the stimulated ear than in the hemisphere contralateral to it (Fig. 5). This indicates that bilateral vestibular cortical projections have two preponderances: in the non-dominant hemisphere and the hemisphere

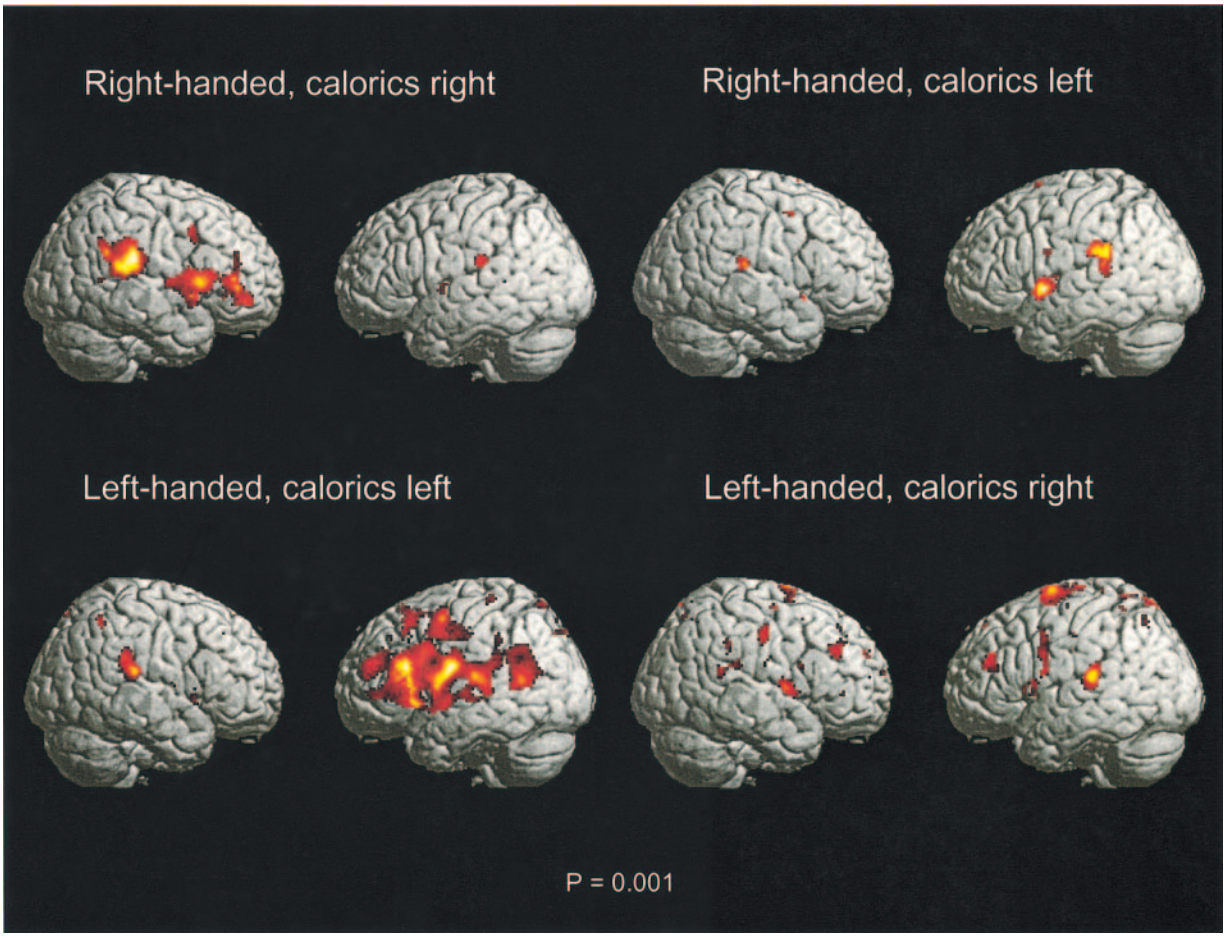

Figure 4. Lateral views of the surfaces of both hemispheres showing activated areas during caloric stimulation of the right or left ear in right- and left-handed volunteers (group analysis; $n = 12$; $P < 0.001$).

ipsilateral to the stimulated ear. These two factors determine the resulting symmetry or asymmetry of the activation pattern during vestibular stimulation, which was also seen during caloric stimulation with iced water (Dieterich *et al.*, 1996). In the following we discuss (i) the anatomical localization of vestibular cortex areas in humans with respect to cortical maps from animal studies and earlier studies in humans, (ii) the vestibular projections to both hemispheres and (iii) the dominance for vestibular cortical function in the non-dominant hemisphere.

Anatomical Localization of Vestibular Cortex Areas in Humans during Vestibular Stimulation

The posterior parts of the insula appeared to be activated in the group analysis under all four stimulation conditions. This area represents the PIVC in humans. It was first described by Grüsser and co-workers (Grüsser *et al.*, 1982, 1990a,b; Guldin and Grüsser, 1996, 1998) in several monkey species and corresponds to findings in feline studies (Jijiwa *et al.*, 1991). Indeed, clinical studies in patients with infarctions of the temporal lobe (Brandt *et al.* 1994, 1995) and activation studies in healthy subjects using vestibular or optokinetic stimuli (Bottini *et al.*, 1994; Bucher *et al.*, 1997; Dieterich *et al.*, 1998) indicate that the posterior insular and retroinsular regions contain the human homologue to the PIVC in monkeys.

During caloric irrigation, a widely distributed pattern of separate areas was activated, including not only the PIVC in the posterior insula, but also the anterior part of the insula, the adjacent superior temporal (BA 42) and transverse temporal gyri, the inferior parietal lobe (BA 40), the anterior cingulum (BA 32, 24), the precuneus (BA 7) and the precentral gyrus (BA 6). All these areas are part of the 'inner vestibular cortical circle' and the core region of the PIVC, which has been electrophysiologically delineated (Guldin and Grüsser, 1996, 1998) in different monkey species. These areas and other vestibular cortex areas such as 2v and 3aV respond to vestibular stimulation. Their neurons are all multisensory, i.e. they also receive visual and/or somatosensory input. They have been found to be intimately connected with each other and with the vestibular brainstem nuclei (Akbarian *et al.*, 1993, 1994; Guldin *et al.*, 1993), where vestibular signals from the semicircular canals and otoliths converge (Angelaki *et al.*, 1993). The PIVC receives input from all these areas, thus enabling it to act as a centre for processing vestibular information as opposed to the concurrent visual (optokinetic) and somatosensory input (Guldin and Grüsser, 1996, 1998).

Does the localization of the calorically activated areas in humans match the cortical distribution of the multisensory vestibular cortex areas identified by single unit recordings in the monkey? In contrast to the precise knowledge of the cortical representation of the vestibular system in electrophysiological animal studies, human data are sparse. Lesion studies in patients with infarctions within the middle cerebral artery territory showed that the retroinsular region around the PIVC affects spatial orientation. Infarctions of this region regularly caused

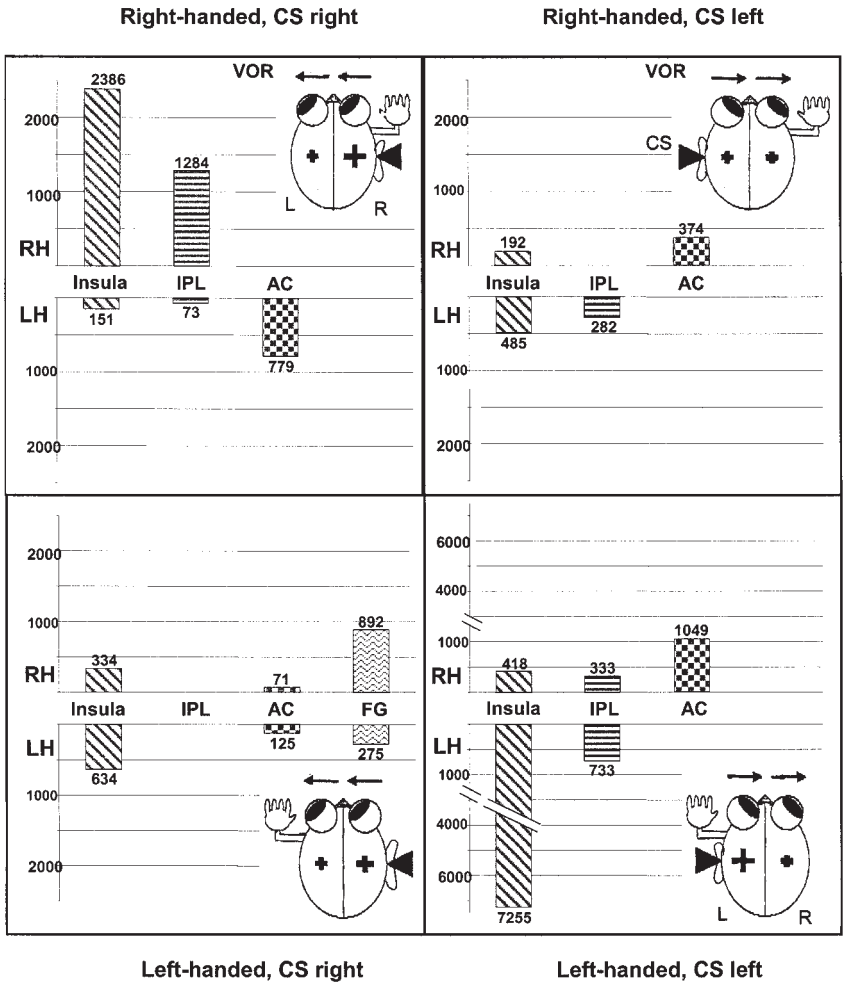

Figure 5. Series of bar graphs for the four stimulation conditions showing the cluster sizes (in voxels) of activated areas in the insula, inferior parietal lobule (IPL), anterior cingulum (AC) and frontal gyri (FG) for both hemispheres, the right (RH) and left hemispheres (LH). The simplified schematic diagrams depict the experimental setup and the main results of activation as approximated by the size of the cross (CS, caloric stimulation 44°C, bold arrow; VOR, direction of slow phase of vestibular nystagmus; R, right side; L, left side).

significant (mostly contra-versive) tilts of adjustments of the perceived visual vertical, best explained as cortical vestibular otolith dysfunction (Brandt *et al.*, 1994; Dieterich and Brandt, 1996). In exceptional cases, transient rotational vertigo was observed in acute infarctions that included this site (Brandt *et al.*, 1995). Earlier human activation studies using vestibular caloric irrigation and PET (Bottini *et al.*, 1994; Dieterich *et al.*, 1996) or vestibular galvanic stimulation at the mastoid level and fMRI (Bucher *et al.*, 1998) confirmed that this location was the presumed PIVC. Galvanic stimulation at the mastoid level stimulates both semicircular canals as well as otolith nerve fibres. It also elicits an activation focus in the first and/or second long insular gyrus (insular gyrus IV and V) of both hemispheres, as indicated by fMRI studies (Bucher *et al.*, 1998; Bense *et al.*, 2001). Thus, the human homologue of the PIVC was found with galvanic (whole vestibular nerve) and caloric (horizontal semicircular canal) stimulation.

Temporo-insular Activation

The temporo-insular activation in the current study extended anteriorly from the long insular gyri to the anterior insula and the adjacent inferior frontal gyrus and posteriorly to retroinsular regions and the superior temporal gyrus. Both areas agree with the activation patterns found in previous imaging studies during galvanic vestibular stimulation (Lobel *et al.*, 1998; Bense *et al.*, 2001). The activated area in the anterior insula and the inferior frontal gyrus in these studies was attributed to simultaneous ocular motor responses mediated by the basal ganglia–thalamo-cortical motor loop described previously (Alexander *et al.*, 1986). The latter was supported by fMRI studies on the differential effects of optokinetic stimulation, since this activity was also suppressed along with optokinetic nystagmus by fixating a stationary target in the centre of the optokinetic pattern (Dieterich *et al.*, 1998). Similarly, our current study with caloric irrigation as well as the study with optokinetic stimulation also found activity in the basal ganglia (putamen, caudate nucleus, substantia nigra) and the thalamus, which probably reflects the efferent motor loop.

Activations of the retroinsular region and the adjacent superior temporal gyrus or transverse temporal gyrus are compatible with a visual and optokinetic region, the visual posterior sylvian area (VPS or VTS), which was originally identified in the monkey (Guldin and Grüsser, 1998). This region was found to be located directly posterior to the PIVC. Because of their adjacent localization, the PIVC and the VPS may be difficult to separate in vestibular activation studies. According to monkey data, the PIVC is considered a vestibular region with optokinetic input and the VPS a visual and optokinetic region

with vestibular input. About one-third of the VPS neurons were driven or modulated by vestibular stimuli (Guldin and Grüsser, 1998).

Parietal Activations

Another neighbouring region of the complex of the PIVC and the VPS is area 7 in the inferior parietal lobule (BA 40), which also receives vestibular input in cats and monkeys (Faugier-Grimaud and Ventre, 1989; Guldin and Grüsser, 1998). Parts of the inferior parietal lobule (BA 40) were also activated in the current study, as well as the cingulum and the precuneus (BA 7), all of which belong to the 'vestibular cortical circuit' in the monkey (Guldin and Grüsser 1996, 1998). These data are compatible with some of the available imaging studies in humans (Bottini *et al.*, 1994; Vitte *et al.*, 1996; Bucher *et al.*, 1998; Lobel *et al.*, 1998; Bense *et al.*, 2001; Suzuki *et al.*, 2001), which allowed for separation of the activation clusters and described a network in the parieto-temporo-occipital junction of vestibularly driven cortex areas similar to that described in monkeys. Among the electrophysiologically determined multi-sensory vestibular areas, area 2v, which is located parietal at the anterior end of the intraparietal sulcus in monkeys (Akbarian *et al.*, 1994; Fredrickson *et al.*, 1966), was not activated in our study. In humans, this area is possibly involved in the control of saccadic eye movements and assigned to the parietal eye field (Müri *et al.*, 1996); it also plays a role in spatial attention during the control of eye movements (Kim *et al.*, 1999).

The activation of the precuneus (BA 7) in the inferior parietal cortex in our study agrees with monkey data that showed anatomic connections of the inferior parietal cortex (area 7) with subcortical structures related to vestibulo-ocular function (Ventre and Faugier-Grimaud, 1986; Faugier-Grimaud and Ventre, 1989). The contribution of the cuneus/precuneus has also been demonstrated in visuo-spatial attention tasks (Corbetta *et al.*, 1993).

Frontal Activations

Activations of the frontal lobe were concentrated especially in the superior (BA 10/8) and medial (BA 9/8/6) frontal gyri, in the diagonal frontal gyrus (BA 6) and the inferior frontal gyrus (BA 44/6) adjacent to the more prominent precentral gyrus/sulcus (BA 6 caudally). Activation of the left inferior Broca's area (BA) 44/6 which extended into the neighbouring insula has been described during rhythm tasks (Platel *et al.*, 1997). Activations in BA 44 and 6 were also reported by Lobel and co-workers (Lobel *et al.*, 1998) during galvanic vestibular stimulation and by Dieterich and co-workers (Dieterich *et al.*, 1998, 2002) during optokinetic nystagmus. Since optokinetic nystagmus and different types of saccades elicited additional activations in rostral parts of the precentral sulcus, corresponding to the location of the frontal eye field (FEF) in the literature, a premotor function of this inferior frontal area has been discussed (Heide *et al.*, 2001; Dieterich *et al.*, 2002). Earlier monkey data (Guldin and Grüsser, 1998), which described a premotor area in area 6 that was tightly connected to the PIVC and the VPS, agree with this view. Our study also has to assume the presence of this premotor area, because the FEF – expected in the vicinity of the precentral sulcus and at the depth of the caudal part of the superior frontal sulcus (Paus, 1996; Petit *et al.*, 1997; Petit and Haxby, 1999) – was also activated. Activation of the FEF is due to the nystagmus elicited by caloric irrigation. Frontal activations might reflect either a feedback signal for the eye position and/or an involvement of spatial attention. In humans, acute lesions of the right dorsolateral prefrontal cortex induce visual neglect (Husain and Kennard, 1996). In monkeys, neuronal activity in the dorsolateral prefrontal cortex was found to be related to saccadic eye movements and attentional tasks (Funahashi *et al.*, 1991).

Anterior Cingulate Activations

Larger activations were located in the anterior cingulum (BA 32, BA 24) predominantly in the hemisphere contralateral to the stimulated ear; the meaning of this lateralization remains unclear. Activations in the hippocampus and anterior cingulate cortex were described earlier during caloric irrigation with cold water (Vitte *et al.*, 1996). This finding is in accordance with other vestibular imaging studies in humans using PET (Bottini *et al.*, 1994; Wenzel *et al.*, 1996) and fMRI (Lobel *et al.*, 1998; Bense *et al.*, 2001) and with monkey data (Guldin and Grüsser, 1996, 1998) in which the anterior cingulate cortex also belongs to the 'inner vestibular circuit'. Activations of the anterior cingulate cortex were also reported to occur during visuo-spatial attention tasks (Corbetta *et al.*, 1993; Kim *et al.*, 1999). Conversely, rostral and caudal regions of the anterior cingulate cortex were activated in PET during oculomotor tasks (direction-specific saccades); their activation was combined with activation of the lateral prefrontal cortex (Paus *et al.*, 1993), which was also found in our study. This localization of task-specific changes of activity within the human anterior cingulate cortex is consistent with the known somatotopic organization of the cingulate cortex in monkeys and confirms the role of the anterior cingulate cortex in the control of motor responses (Paus *et al.*, 1993). Thus, further discussion of cortical and subcortical activations due to vestibular stimulation must bear in mind that perceptual, sensorimotor (ocular and body) and autonomic functions are involved.

Cortico-cortical and Cortico-subcortical Connections of Vestibular Cortex Areas

Neurophysiologically, the main input from the vestibular nuclei in the brainstem to the cortical PIVC in monkeys travels via the ventroposterior thalamic subnuclei, especially the posterior part of the ventroposterior nucleus and the medial pulvinar (Akbarian *et al.*, 1992). Both areas, thalamus and midbrain, were activated in our study. These vestibular thalamic subnuclei in non-human primates are directly connected to three vestibular cortical regions – the PIVC, area 2v (7ant) and the 'proprioceptive vestibular' area 3aV – and have strong bilateral interconnections (Guldin and Grüsser, 1996). As mentioned previously, animal studies have identified several additional regions with strong bilateral connections to this inner vestibular cortical circle, namely the cingulate sulcus, the post arcuate area 6 (6pa), the granular insular region, parts of area 7 and a temporal region adjacent to the PIVC called the VPS or VTS (Guldin and Grüsser, 1996, 1998). The vestibular brainstem nuclei receive monosynaptic input from all the above-mentioned cortex regions and an area inside the cingular sulcus (Akbarian *et al.*, 1993, 1994; Guldin *et al.*, 1993). Thus, the same cortical regions that have efferent connections to the PIVC also have efferent monosynaptic connections to the vestibular nuclei. These cortico-vestibular projections run to both the ipsilateral and contralateral vestibular brainstem nuclei. However, the contribution of ipsilateral and contralateral cortical areas varies for the different cortex areas (Guldin and Grüsser, 1996). The PIVC, VTS and granular insula preferably project to and from the ipsilateral vestibular nuclei, whereas the premotor area 6, the somatosensory areas 3aV and 3aH, and area 2v have more pronounced projections to the contralateral vestibular nuclei

(Akbarian *et al.*, 1993, 1994; Guldin *et al.*, 1993). Thus, the ipsilateral projection to and from the PIVC and the adjacent VTS can explain one finding of our activation study during caloric irrigation: the importance of the side of the stimulated ear, i.e. the activation was stronger in the posterior insula ipsilateral to the stimulated ear.

Dominance of Vestibular Function of the Non-dominant Hemisphere

The cortex areas with vestibular input were activated bilaterally in all right-handed healthy volunteers, but there was a significant preponderance of the non-dominant right hemisphere in our study. The 12 healthy volunteers with strong left-handedness exhibited an analogous predominance of activation in their left hemisphere. The latter was not only evident in group analysis, but also in single subject analysis. Thus, the dominance for vestibular cortex activation of the non-dominant hemisphere is more regularly found than hemispheric transposition for Broca's area in left-handed subjects. It has been reported that 60% of the right-handed, but only 32% of the non-right-handed, developed aphasia after left hemisphere lesions (Benson and Geschwind, 1985). This finding contradicts that of the first PET study during vestibular stimulation (Bottini *et al.*, 1994), which found widespread activations in the temporo-parietal cortex during caloric irrigation in the hemisphere contralateral to the irrigated ear. However, this study did not systematically compare right and left ear irrigation in the same subject and used iced water for caloric irrigation. Such a painful stimulus probably led to a concurrent stimulation of the nociceptive and somatosensory systems in the contralateral hemisphere. This was confirmed by the finding that somatosensory areas of the perisylvian cortex, the temporo-parietal junction and somatosensory area II received signals from both sensory channels: the one was activated during caloric vestibular stimulation with iced water and the other, during mechanical vibration of posterior neck muscles (Bottini *et al.*, 2001).

A significant right hemispheric dominance for vestibular cortex areas in the temporo-insular-parietal region was reported earlier in an fMRI study using optokinetic stimulation (Dieterich *et al.*, 1998). This dominance was also described in the dipole analysis of a magnetoencephalography study for the processing of sound-source lateralization (Kaiser *et al.*, 2000). The lateralized effects were localized bilaterally over the angular gyri and posterior temporal regions. During optokinetic stimulation, a right hemispheric dominance was also detected for cortical ocular motor areas (parietal cortex with PEF) and motion-sensitive areas (MT/MST), but not for the primary visual cortex (Dieterich *et al.*, 1998). This agrees with other paradigms showing right hemispheric predominance for the areas FEF and SMA during memory-guided saccades after a delay period, using PET (Sweeney *et al.*, 1996), for the PEF during visually guided saccades, using fMRI (Müri *et al.,* 1996) and for the middle frontal gyrus, which corresponds to Brodmann's area 46, in a spatial working memory task, using fMRI (McCarthy *et al.,* 1996). Similarly, PET activation in the anterior temporal lobe (midway along the superior temporal sulcus) was clearly stronger in the right hemisphere for selective attention during visual discrimination of shape, but not of speed and colour (Corbetta *et al.*, 1991) and in the infero-temporal cortex for several object recognition tasks (Corbetta *et al.,* 1990). Petrides and co-workers (Petrides *et al.*, 1993) reported strong right lateralization in the mid-dorsolateral frontal cortex (BA 46) when subjects were asked to point to spatially arranged designs. The latter task – in our opinion – requires vestibularly defined coordinates. Another PET study on attention (Pardo *et al.*, 1991) found predominant activation in the right prefrontal and superior parietal cortex independently of the laterality and modality of the sensory input. Finally, patients with chronic lateralized ongoing pain (painful mononeuropathy) showed a striking preferential activation of the right anterior cingulate cortex (BA 24), regardless of the side of the mononeuropathy, which suggests a right hemispheric lateralization for affective processing (Hsieh *et al.*, 1995).

Clinical lesion studies have shown a right hemispheric predominance in patients with parietal lesions that typically cause visuospatial hemineglect (Vallar and Perani, 1986). With respect to eye movements, smooth pursuit was more severely impaired in patients with lesions involving the right posterior parietal cortex and/or dorsolateral frontal cortex than the left (Lekwuwa and Barnes, 1996). A clinical study on direction-specific pursuit defects and impairment of motion perception in unilateral hemispheric lesions found that two of three patients with left hemispheric lesions had bidirectional defects in motion discrimination, but none of the 21 patients with right-sided lesions had bidirectional deficits (Barton *et al.*, 1996). All these data are compatible with the model of Mesulam (Mesulam, 1981, 1999), which describes a network for representing and exploring space for which right-handed subjects have a right hemispheric dominance. On the whole, all these studies indicate that functionally significant right hemispheric dominance must be assumed for visuo-spatial orientation and attention, motion perception, saccadic and pursuit eye movements and, especially, for the processing of vestibular function. These functions have in common a multisensory and motor processing of spatial coordinates in three dimensions. The vestibular system with otolith and semicircular canal input is an important, integral part and, hence, is involved not only in the perception of body position and self-motion, but also in attention and the control of ocular motor, head and body movements (a dysfunction of which, for example, causes visuo-spatial hemineglect).

For all the above-discussed sensorimotor functions there are no studies available on left-handers. This makes it difficult to interpret the function of our finding of left hemispheric vestibular dominance in left-handers. The two functions – sensorimotor control of fine finger and arm movements and spatial orientation with ocular motor and postural control – are mediated in both hemispheres; however, their dominance seems to be organized in opposite hemispheres. Whereas orientation, ocular motor and postural control represent more ancient sensorimotor functions developed during evolution, speech and finger movements are more recent achievements. The preference of hemispheres may thus be a product of evolution. One could speculate that there are phylogenetic and ontogenetic determinants of hemispheric dominance. The 'ancient' vestibular system matures earlier during ontogenetic development. This can be demonstrated by postural neck and vestibulo-ocular reflexes that are present shortly after birth. In contrast, handedness and language lateralization seem to develop a few years later. For example, left hemisphere lateralization of receptive language is present at the age of 8 years (Balsamo *et al.*, 2002). There are two possible explanations for the opposite hemispherical dominance: first, that the side of dominance of the vestibular system determines later handedness during maturation of motor function in childhood or, secondly, that an as yet unknown constellation determines both handedness and vestibular hemispherical dominance in the two hemispheres. The dominance of vestibular cortical function should not be simply limited to the vestibular sense *per se*, but rather should

be seen as part of a multisensory and sensorimotor cortical interaction to ensure the perception of gravity and motion and the maintenance of equilibrium. There is no primary vestibular cortex like the visual cortex. All vestibular cortical neurons identified electrophysiologically in monkeys also responded to other sensory and optokinetic stimuli (Grüsser *et al.*, 1990a,b; Guldin and Grüsser, 1996). The cytoarchitectonic structure of the vestibular cortex areas is also more typical of a multisensory or sensorimotor rather than a unimodal sensory cortex. Indeed, the vestibular cortex contributes to a complex multi-purpose network for detection, interpretation and motor reaction to changes in egocentric space.

Conclusion

In summary, there is convincing evidence that the multisensory neuronal assembly in the posterior insula represents the PIVC in both humans and non-human primates. It receives sensory input from vestibular, visual and somatosensory systems. Patients with acute infarctions of the PIVC regularly present with static vestibular dysfunction (tilts of the perceived verticality) and rarely with associated rotatory vertigo. Vestibular signals from the semicircular canals and the otoliths converge at the level of the vestibular nuclei and project to the same cortical loci by ipsilateral and contralateral ascending pathways to both hemispheres. This PET study has, with the use of caloric irrigation, disclosed two functional dominances for the processing of vestibular information: first, the dominance of the non-dominant hemisphere and, secondly, the dominance of the hemisphere ipsilateral to the irrigated ear. It is possible that the vestibular system – which matures earlier ontogenetically – and its hemispherical dominance determine handedness.

Notes

This work was supported by the Wilhelm Sander-Stiftung and the German Research Foundation (DFG: Di 379/4-1; Br 639/6-1). We are grateful to Judy Benson for critically reading the manuscript and to the anonymous referee for designing the inserted diagrams in Figure 5.

Address correspondence to Prof. Dr Marianne Dieterich, Department of Neurology, Johannes Gutenberg University of Mainz, Langenbeckstrasse 1, D-61377 Mainz, Germany. Email: dieterich@neurologie.klinik.uni-mainz.de.

References

Akbarian S, Grüsser O-J, Guldin WO (1992) Thalamic connections of the vestibular cortical fields in the squirrel monkey (*Saimiri sciureus*). J Comp Neurol 325:1–19.

Akbarian S, Grüsser O-J, Guldin WO (1993) Corticofugal projections to the vestibular nuclei in the squirrel monkey: further evidence of multiple cortical vestibular fields. J Comp Neurol 332:89–104.

Akbarian S, Grüsser O-J, Guldin WO (1994) Corticofugal connections between the cerebral cortex and brainstem vestibular nuclei in the macaque monkey. J Comp Neurol 339:421–437.

Alexander GE, DeLong MR, Strick PL (1986) Parallel organization of functionally segregated circuits linking basal ganglia and cortex. Annu Rev Neurosci 9:357–381.

Angelaki DE, Bush GA, Perachio AA (1993) Two-dimensional spatiotemporal coding of linear acceleration in vestibular nuclei neurons. J Neurosci 13:1403–1417.

Balsamo LM, Xu B, Grandin CB, Petrella JR, Braniecki SH, Elliott TK, Gaillard WD (2002) A functional magnetic resonance imaging study of left hemisphere language dominance in children. Arch Neurol 59:1168–1174.

Barton JJS, Sharpe JA, Raymond JE (1996) Directional defects in pursuit and motion perception in humans with unilateral lesions. Brain 119:1535–50.

Bense S, Stephan T, Yousry TA, Brandt T, Dieterich M (2001) Multisensory cortical signal increases and decreases during vestibular galvanic stimulation (fMRI). J Neurophysiol 85:886–899.

Benson DF, Geschwind N (1985) Aphasia and related disorders: a clinical approach. In: Principles of behavioral neurology (Mesulam MM, ed.), pp. 193–238. Philadelphia: PA Davis.

Boecker H, Ceballos-Baumann A, Bartenstein P, Weindl A, Siebner HR, Faßbender T, Munz F, Schwaiger M, Conrad B (1999) Sensory processing in Parkinson's and Huntington's disease: investigation with 3D H2O15-PET. Brain 122:1651–1665.

Bottini G, Sterzi R, Paulesu E, Vallar G, Cappa SF, Erminio F, Passingham RE, Frith CD, Frackowiak RSJ (1994) Identification of the central vestibular projections in man: a positron emission tomography activation study. Exp Brain Res 99:164–169.

Bottini G, Karnath HO, Vallar G, Sterzi R, Frith CD, Frackowiak RSJ, Paulescu E (2001) Cerebral representations for egocentric space. Functional-anatomical evidence from caloric vestibular stimulation and neck vibration. Brain 124:1182–1196.

Brandt T, Dieterich M, Danek A (1994) Vestibular cortex lesions affect the perception of verticality. Ann Neurol 35:403–412.

Brandt T, Bötzel K, Yousry T, Dieterich M, Schulze S (1995) Rotational vertigo in embolic stroke of the vestibular and auditory cortices. Neurology 45:42–44.

Bucher SF, Dieterich M, Seelos KC, Brandt T (1997) Sensorimotor cerebral activation during optokinetic nystagmus: a functional MRI study. Neurology 49:1370–1377.

Bucher SF, Dieterich M, Wiesmann M, Weiss A, Zink R, Yousry T, Brandt T (1998) Cerebral functional MRI of vestibular, auditory, and nociceptive areas during galvanic stimulation. Ann Neurol 44:120–125.

Büttner U, Buettner UW (1978) Parietal cortex area 2 V neuronal activity in the alert monkey during natural vestibular and optokinetic stimulation. Brain Res 153:392–397.

Corbetta M, Miezin FM, Dobmeyer S, Shulman GL, Petersen SE (1990) Attention modulation of neural processing of shape, color, and velocity in humans. Science 248:1556–1559.

Corbetta M, Miezin FM, Dobmeyer S, Shulman GL, Petersen SE (1991) Selective and divided attention during visual discriminations of shape, color and speed: functional anatomy by positron emission tomography. J Neurosci 11:2383–2402.

Corbetta M, Miezin FM, Gordon L, Shulman GL, Petersen SE (1993) A PET study of visuospatial attention. J Neurosci 13:1202–1226.

Dieterich M, Brandt T (1996) Perceived vertical in patients with cortical stroke. In: Le cortex vestibulaire (Collard M, Jeannerod M, Christen Y, eds), pp. 83–94. Paris: Ipsen, Editions IRVINN.

Dieterich M, Brandt T, Bartenstein P, Wenzel R, Danek A, Lutz S, *et al.* (1996) Different vestibular cortex areas activated during caloric irrigation: a PET study. J Neurol 243:40.

Dieterich M, Bucher SF, Seelos KC, Brandt T (1998) Horizontal or vertical optokinetic stimulation activates visual motion-sensitive, ocular motor, and vestibular cortex areas with right hemispheric dominance: an fMRI study. Brain 121:1479–1495.

Dieterich M, Bense S, Stephan T, Yousry TA, Brandt T (2003) fMRI signal increases and decreases in cortical areas during small-field optokinetic stimulation and central fixation. Exp Brain Res 147:117–127.

Drzezga A, Darsow U, Treede R-D, Siebner H, Frisch M, Munz F, Weilke F, Ring J, Schwaiger M, Bartenstein P (2001) Central activation by histamine-induced itch: analogies to pain processing. A correlational analysis of O-15 H_2O PET-studies. Pain 92:295–305.

Faugier-Grimaud S, Ventre J (1989) Anatomic connections of inferior parietal cortex (area 7) with subcortical structures related to vestibulo-ocular function in a monkey (*Macaca fascicularis*). J Comp Neurol 280:1–14.

Frackowiak RSJ, Friston KJ, Frith CD, Dolan R, Mazziotta JC (1997) Human brain function. London: Academic Press.

Fredrickson JM, Figge U, Scheid P, Kornhuber HH (1966) Vestibular nerve projection to the cerebral cortex of the rhesus monkey. Exp Brain Res 2:318–327.

Friberg L, Olsen TS, Roland PE, Paulson OB, Lassen NA (1985) Focal increase of blood flow in the cerebral cortex of man during vestibular stimulation. Brain 108:609–623.

Frison L, Popcock S (1992) Repeated measures in clinical trials: analysis using mean summary statistics and its implications for design. Stat Med 11:1685–1704.

Friston KJ, Holmes AP, Worsley K, Poline J-B, Frith C, Frackowiak RSJ (1995a) Statistical parametric maps in functional imaging: a general linear approach. Hum Brain Mapp 2:189–210.

Friston KJ, Holmes AP, Poline JB, Grasby BJ, Williams CR, Frackowiak RSJ,

Turner R (1995b) Analysis of fMRI time-series revisited. Neuroscience 2:45–53.
Funahashi S, Bruce CJ, Goldman-Rakic PS (1991) Neuronal activity related to saccadic eye movements in the monkey's dorsolateral prefrontal cortex. J Neurophysiol 65:1464–1483.
Grüsser OJ, Pause M, Schreiter U (1982) Neuronal responses in the parieto insular vestibular cortex of alert Java monkeys (*Macaca fascicularis*). In: Physiological and pathological aspects of eye movements (Roucoux A, Crommelink M, eds), pp. 251–270. The Hague: W. Junk.
Grüsser OJ, Pause M, Schreiter U (1990a) Vestibular neurons in the parieto-insular cortex of monkeys (*Macaca fascicularis*). Visual and neck receptor responses. J Physiol 430:559–583.
Grüsser OJ, Pause M, Schreiter U (1990b) Localization and responses of neurons in the parieto-insular vestibular cortex of awake monkeys (*Macaca fascicularis*). J Physiol 430:537–557.
Guldin WO, Grüsser OJ (1996) The anatomy of the vestibular cortices of primates. In: Le cortex vestibulaire (Collard M, Jeannerod M, Christen Y, eds), pp. 17–26. Paris: Ipsen, Editions IRVINN.
Guldin WO, Grüsser O-J (1998) Is there a vestibular cortex? Trends Neurosci 21:254–259.
Guldin WO, Mirring S, Grüsser O-J (1993) Connections from the neocortex to the vestibular brain stem nuclei in the common marmoset. Neuroreport 5:113–116.
Heide W, Binkofski F, Seitz RJ, Posse S, Nitschke MF, Freund HJ, Kömpf D (2001) Activation of frontoparietal cortices during memorized triple-step sequences of saccadic eye movements: an fMRI study. Eur J Neurosci 13:1177–1189.
Hsieh J-C, Belfrage M, Stone-Elander S, Hansson P, Ingvar M (1995) Central representation of chronic ongoing neuropathic pain studied by positron emission tomography. Pain 63:225–236.
Husain M, Kennard C (1996) Visual neglect associated with frontal lobe infarction. J Neurol 243:652–657.
Jijiwa H, Kawaguchi T, Watanabe S, Miyata H (1991) Cortical projections of otolith organs in the cat. Acta Otolaryngol (Stockh) 481(Suppl.):69–72.
Kaiser J, Lutzenberger W, Preissl H, Ackermann H, Birbaumer N (2000) Right-hemisphere dominance for the processing of sound-source lateralization. J Neurosci 20:6631–6639.
Kim YH, Gitelman DR, Nobre AC, Parrish TB, LaBar KS, Mesulam MM (1999) The large-scale neural network for spatial attention displays multifunctional overlap but differential asymmetry. Neuroimage 9:269–277.
Lekwuwa GU, Barnes GR (1996) Cerebral control of eye movements. The relationship between cerebral lesion sites and smooth pursuit deficits. Brain 119:473–490.
Lobel E, Kleine JF, Le Bihan D, Leroy-Willig A, Berthoz A (1998) Functional MRI of galvanic vestibular stimulation. J Neurophysiol 80:2699–2709.
McCarthy G, Puce A, Constable RT, Krystal JH, Gore JC, Goldman-Rakic P (1996) Activation of human prefrontal cortex during spatial and nonspatial working memory tasks measured by functional MRI. Cereb Cortex 6:600–611.
Mesulam MM (1981) A cortical network for directed attention and unilateral neglect. Ann Neurol 10:309–325.
Mesulam MM (1999) Spatial attention and neglect: parietal, frontal and cingulated contributions to the mental representation and attentional targeting of salient extrapersonal events. Philos Trans R Soc Lond B Biol Sci 354:1325–1246.
Müri RM, Iba-Zizen MT, Derosier C, Cabanis C, Pierrot-Deseilligny C (1996) Location of the human posterior eye field with functional magnetic resonance imaging. J Neurol Neurosurg Psychiatry 60:445–448.
Naidich TP, Brightbill TC (1996) Systems for localizing fronto-parietal gyri and sulci on axial CT and MRI. Int J Neuroradiol 2:313–338.
Oldfield RC (1971) The assessment and analysis of handedness: the Edinburgh inventory. Neuropsychologia 9:97–113.
Ödkvist LM, Schwarz DWF, Fredrickson JM, Hassler R (1974) Projection of the vestibular nerve to the area 3a arm field in the squirrel monkey (*Saimiri sciureus*). Exp Brain Res 21:97–105.
Pardo JV, Fox PT, Raichle ME (1991) Localization of a human system for sustained attention by positron emission tomography. Nature 349:61–64.
Paus T (1996) Location and function of the human frontal eye-field: a selective review. Neuropsychologica 34:475–483.
Paus T, Petrides M, Evans AC, Meyer E (1993) Role of the human anterior cingulate cortex in the control of oculomotor, manual, and speech responses: a positron emission tomography study. J Neurophysiol 70:453–469.
Petit L, Haxby JV (1999) Functional anatomy of pursuit eye movements in humans as revealed by fMRI. J Neurophysiol 81:463–471.
Petit L, Clark VP, Ingeholm J, Haxby JV (1997) Dissociation of saccade related and pursuit related activation in human frontal eye fields as revealed by fMRI. J Neurophysiol 77:3386–3390.
Petrides M, Alivisatos B, Evans AC, Meyer E (1993) Dissociation of human mid-dorsolateral from posterior dorsolateral frontal cortex in memory processing. Proc Natl Acad Sci USA 90:873–877.
Phillips CG, Powell TPS, Wiesendanger M (1971) Projection from low threshold muscle afferents of hand and forearm to area 3a of Baboon's cortex. J Physiol (Lond) 217:419–446.
Platel H, Price C, Baron JC, Wise R, Lambert J, Frackowiak RSJ, Lechevalier B, Eustache F (1997) The structural components of music perception. A functional anatomical study. Brain 120:229–243.
Salmaso D, Longoni AM (1985) Problems in the assessment of hand preference. Cortex 21:533–549.
Schwarz DWF, Fredrickson JM (1971) Rhesus monkey vestibular cortex: a bimodal primary projection field. Science 172:280–281.
Schwarz DWF, Deecke L, Fredrickson JM (1973) Cortical projection of group I muscle afferents to areas 2, 3a and the vestibular field in the rhesus monkey. Exp Brain Res 17:516–526.
Spence SA, Brooks DJ, Hirsch SR, Liddle PF, Meehan J, Grasby PM (1997) A PET study of voluntary movement in schizophrenic patients experiencing passivity phenomena (delusions of alien control). Brain 120:1997–2011.
Stephan KM, Schüller M, Höflich P, Knorr U, Binkofski F, Seitz RJ (1997) Normalization into Talairach space: variability of reference coordinates. Neuroimage 5:S416.
Suzuki M, Kitano H, Ito R, Kitanishi T, Yazawa Y, Ogawa T, Shiino A, Kitajima K (2001) Cortical and subcortical vestibular response to caloric stimulation detected by functional magnetic resonance imaging. Cog Brain Res 12:441–449.
Sweeney JA, Mintun MA, Kwee S, Wiseman MB, Brown DL, Rosenberg DR, *et al.* (1996) Positron emission tomography study of voluntary saccadic eye movements and spatial working memory. J Neurophysiol 75:454–468.
Talairach J, Tournoux P (1988) Co-planar stereotaxic atlas of the human brain. Stuttgart: Thieme.
Takeda N, Hashikawa K, Moriwaki H, Oku N, Koizuka I, Kitahara T, Taya N, Kubo T, Nishimura T (1996) Effects of caloric vestibular stimulation on parietal and temporal blood flow in human brain: a consecutive technetium-99m-HMPAO Spect study. J Vest Res 6:127–134.
Vallar G, Perani D (1986) The anatomy of unilateral neglect after right hemisphere stroke lesions: a clinical CT correlation study in man. Neuropsychologia 24:609–622.
Ventre J, Faugier-Grimaud S (1986) Effects of posterior parietal lesions (area 7) on VOR in monkeys. Exp Brain Res 62:654–658.
Vitte E, Derosier C, Caritu Y, Berthoz A, Hasboun D, Soulie D (1996) Activation of the hippocampal formation by vestibular stimulation: a functional magnetic resonance imaging study. Exp Brain Res 112:523–526.
Wenzel R, Bartenstein P, Dieterich M, Danek A, Weindl A, Minoshima S, Ziegler S, Schwaiger M, Brandt T (1996) Deactivation of human visual cortex during involuntary ocular oscillations. A PET activation study. Brain 119:101–110.
Woods RP (1996) Modeling for intergroup comparisons of imaging data. Neuroimage 4:84–94.
Yousry TA, Fesl G, Büttner A, Noachtar S, Schmid DU, Peraud A, Winkler P (1997) Heschl's gyrus: anatomic description and methods of identification in MRI. Int J Neuroradiol 3:2–12.